MOLECULAR AND CELLULAR BIOLOGY, July 2000, p. 4614–4625 Vol. 20, No. 13
0270-7306/00/$04.00+0

Hsl1p, a Swe1p Inhibitor, Is Degraded via the Anaphase-Promoting Complex

JANET L. BURTON AND MARK J. SOLOMON*

Department of Molecular Biophysics & Biochemistry, Yale University, New Haven, Connecticut 06520-8114

Received 24 November 1999/Returned for modification 10 January 2000/Accepted 15 March 2000

Ubiquitination and subsequent degradation of critical cell cycle regulators is a key mechanism exploited by the cell to ensure an irreversible progression of cell cycle events. The anaphase-promoting complex (APC) is a ubiquitin ligase that targets proteins for degradation by the 26S proteasome. Here we identify the Hsl1p protein kinase as an APC substrate that interacts with Cdc20p and Cdh1p, proteins that mediate APC ubiquitination of protein substrates. Hsl1p is absent in G_1, accumulates as cells begin to bud, and disappears in late mitosis. Hsl1p is stabilized by mutations in *CDH1* and *CDC23*, both of which result in compromised APC activity. Unlike Hsl1p, Gin4p and Kcc4p, protein kinases that have sequence homology to Hsl1p, were stable in G_1-arrested cells containing active APC. Mutation of a destruction box motif within Hsl1p ($Hsl1p^{db\text{-}mut}$) stabilized Hsl1p. Interestingly, this mutation also disrupted the Hsl1p-Cdc20p interaction and reduced the association between Hsl1p and Cdh1p in coimmunoprecipitation studies. These findings suggest that the destruction box motif is required for Cdc20p and, to a lesser extent, for Cdh1p to target Hsl1p to the APC for ubiquitination. Hsl1p has been previously shown to inhibit Swe1p, a protein kinase that negatively regulates the cyclin-dependent kinase Cdc28p, by promoting Swe1p degradation via SCF^{Met30} in a bud morphogenesis checkpoint. Results of the present work indicate that Hsl1p is degraded in an APC-dependent manner and suggest a link between the SCF (Skp1-cullin-F box) and APC-proteolytic systems that may help to coordinate the proper progression of cell cycle events.

Cell cycle events must occur in a precise and linear fashion to ensure that the appropriate complement of genetic material and cellular components are equally distributed between daughter cells. In eukaryotes, cell cycle progression is controlled primarily by the activation and inactivation of the cyclin-dependent kinases (Cdks) (40, 52, 58, 65). Activation is achieved both by binding of a cyclin regulatory subunit and by activating phosphorylation by the Cdk-activating kinase (35). Cdks are inactivated by binding of inhibitory proteins, inhibitory phosphorylation of the Cdk (65, 66), and ubiquitin-mediated degradation of the cyclin (38, 78).

In the budding yeast, *Saccharomyces cerevisiae*, cell cycle progression is driven by a single Cdk subunit, Cdc28p, that binds distinct cyclin subunits as cells progress through the division cycle (54). Cdc28p associates with the G_1 cyclins, Cln1p-Cln3p, as cells initiate budding and cell division; with Clb5p and Clb6p, triggering DNA replication; and with the mitotic cyclins, Clb1p to Clb4p, during G_2/M. Cdc28p undergoes activating phosphorylation on Thr-169 by Cak1p (18, 36, 71) and inhibitory phosphorylation on Tyr-19 by Swe1p (6, 45). Although the inhibitory phosphorylation of Cdc28p by Swe1p does not occur in unperturbed cells (3, 67), this phosphorylation does delay the cell cycle in G_2 in response to improper bud formation in a morphogenesis checkpoint pathway (45, 62). Swe1p in turn is negatively regulated by the Hsl1p protein kinase (4, 48, 70). In *hsl1*Δ cells, Swe1p activity prevails, leading to a G_2 delay and an elongated bud morphology due to low levels of Clb-Cdc28p activity (4, 48). Hsl1p appears to be active only when colocalized with the septins (4), cytoskeletal proteins encircling the bud neck. Presumably, Hsl1p localization to properly assembled septins at the bud neck activates it so that it can then inhibit Swe1p and allow cells to proceed to mitosis (4). However, whether Hsl1p phosphorylates Swe1p and whether such phosphorylation inhibits Swe1p activity are currently unknown. Recently, McMillan et al. (50) demonstrated that Hsl1p promotes the degradation of Swe1p, suggesting that Hsl1p inactivates Swe1p via ubiquitin-mediated protein degradation (see below).

Cell cycle progression is also controlled in yeast and higher eukaryotes by ubiquitin-mediated protein degradation of key cell cycle regulators. Ubiquitination of protein substrates and subsequent degradation by the 26S proteasome is required for the initiation of DNA replication, the onset of anaphase, and the exit from mitosis (38, 57, 78). The ubiquitin degradation pathway is a multistep process in which a 76-amino-acid peptide, ubiquitin, is covalently attached to a protein substrate by a series of enzymatic reactions involving a ubiquitin-activating enzyme (E1), a ubiquitin-conjugating enzyme (E2), and, in many cases, a ubiquitin ligase (E3) (29). Proteins that undergo multiple rounds of ubiquitination are then targeted for degradation by the 26S proteasome, a large multicatalytic protease machine (28). Ubiquitin ligases confer substrate specificity to the ubiquitination reaction, consistent with the diversity of E3 enzymes and the complexity of the subunits that comprise them.

One class of ubiquitin ligases that controls cell cycle progression in yeast and higher eukaryotes are the SCFs (Skp1-cullin-F box, for the components that comprise this family of E3s). Different SCF complexes have common Skp1-cullin subunits but distinct F-box proteins (44, 56, 57) that contain either a WD40 or leucine-rich repeat domain that is critical for substrate binding. Thus, the F-box subunit determines the substrate specificity of the SCF E3 (44, 56, 57). In *S. cerevisiae*, the Cdc28p kinase inhibitor, Sic1p, and the G_1 cyclins, Cln1p and Cln2p, are polyubiquitinated by SCF^{Cdc4} (21, 63, 73) and SCF^{Grr1} (15, 64), respectively, as cells progress from G_1 to S

* Corresponding author. Mailing address: Department of Molecular Biophysics & Biochemistry, Yale University, 266 Whitney Ave., New Haven, CT 06520-8114. Phone: (203) 436-4388. Fax: (203) 432-3104. E-mail: Mark.Solomon@Yale.edu.

phase. Swe1p has recently been found to be ubiquitinated by SCF^{Met30}, leading to Swe1p degradation and progression into mitosis (34).

Another major E3 is a multisubunit complex known as the anaphase-promoting complex (APC) or cyclosome (41, 69, 80), which is responsible for ubiquitinating the anaphase inhibitor Pds1p, thus triggering chromosome segregation (10, 11, 13, 76, 77, 81). The APC also ubiquitinates Geminin, a human DNA replication inhibitor that is degraded during anaphase onset (49), Ase1p, a protein involved in mitotic spindle stability in yeast (33), and the mitotic cyclins (14, 31, 32, 39, 41, 60, 79). Proteins that are ubiquitinated by the APC have been shown to contain one or more destruction box sequences, 9-amino-acid motifs with the consensus sequence RXXLXXXXN, where the RXXL is highly conserved (24).

APC activity itself is regulated, being active from anaphase onset through G_1 but then inactive in S, G_2, and early M phases (1, 2, 7, 32). Cdc20p and Cdh1p (also called Hct1p) are WD40 domain proteins that bind to and activate the APC (19, 42, 43, 79). These subunits, like the F-box proteins for SCF complexes, confer substrate specificity to the E3 enzyme, in this case the APC (60, 75). In G_1, Cdc20p promotes the degradation of Pds1p (75) whereas Cdh1p directs the destruction of Ase1p and Clb2p (60, 75). However, in mitosis the substrate specificity of Cdc20p is not as clear, and it appears capable of targeting cyclins for APC-mediated ubiquitination (14, 46, 72, 75). Recently, Cdc20p has been shown to target Clb5p for degradation (61).

In an effort to identify new APC substrates, and thus important cell cycle regulators, we used Cdc20p as the bait protein in a yeast two-hybrid screen and identified Hsl1p. We found that Hsl1p levels oscillate in a cell cycle-dependent manner, being absent in G_1, when APC activity is high, and present in mitosis, when APC activity is low. Hsl1p is stabilized in G_1 by mutations that inactivate the APC and by mutations in a destruction box motif of Hsl1p. Furthermore, in coimmunoprecipitation studies we demonstrated that the destruction box motif of Hsl1p is required for interaction with Cdc20p and to a lesser extent with Cdh1p. These findings, together with genetic studies presented here, suggest that Hsl1p is a substrate but not a direct regulator of APC activity. Previous work had demonstrated that Hsl1p can promote the degradation of the SCF substrate Swe1p; therefore, Hsl1p provides a link between the APC- and SCF-mediated proteolytic systems during cell division.

MATERIALS AND METHODS

Yeast strains and plasmid construction. Yeast strains and their relevant genotypes are shown in Table 1. All strains are derivatives of W303A (*ade2-1 trp1-1 leu2-3,112 his3-11,15 ura3-1 can1-100*) with the exception of K3413 (2) and MaV103 (74), whose complete genotypes are listed in Table 1. Yeast transformations were performed as described previously (22). Genetic manipulations were performed by published methods (26). All PCR products were sequenced to verify that no extraneous mutations were introduced. Underlined residues in oligonucleotides correspond to restriction sites unless otherwise indicated.

The *CDC20*-pAS2 plasmid used in the yeast two-hybrid screen was created by PCR amplification of *CDC20* from pMM45 (a gift from Daniel Burke, University of Virginia, Charlottesville, Va.) using primers MSO519 (5′-CCC/CAT/ATG/CCA/GAA/AGC/TCT/AGA/GAT/AAG-3′) and MSO522 (5′-CCC/GTC/GAC/CCT/GAT/CAA/ATA/TTG/GCT/GG-3′), and was ligated into the pAS2 vector (27) (a gift from Steven Elledge, Baylor College of Medicine, Houston, Tex.) using the *Nde*I and *Sal*I sites (underlined). *CDH1*-pAS2 was constructed by PCR amplification of *CDH1* using the primers MSO604 (5′-CCC/GAA/TTC/GAA/TGT/CCA/CAA/ACC/TG-3′) and MSO605 (5′-CCC/CTC/GAG/CTC/TAA/CGT/ATT/TGA/TT-3′). The amplified *CDH1* was cut with *Eco*RI, filled in, and then cut with *Sal*I to create an in-frame fusion with the Gal4 DNA-binding domain sequence using the *Sma*I and *Sal*I sites of pAS2. *HSL1*-pACTII was created by cutting *GAL-HSL1-HA*-YIplac204 (see below) with *Bam*HI and *Hin*dIII to isolate the entire coding sequence of *HSL1*. The ends of *HSL1* were then filled using Klenow and ligated to the pACTII vector that had been digested with *Bam*HI and filled in with Klenow. $HSL1^{K110A}$-pACTII was constructed by swapping an internal 1.4-kb *Bgl*I-*Avr*II fragment of *HSL1* from pYB123 (a gift from Yves Barral, Yale University, New Haven, Conn.) encoding the K110A mutation with the corresponding fragment from wild-type *HSL1*-pACTII. The pSE1111 plasmid containing *SNF4* fused to the *GAL4* activation domain and the yeast cDNA library containing *GAL4* activation domain fusions were gifts from Steven Elledge (27).

The *HSL1-HA*-YIplac211 and *HSL1-HA*-YIplac204 constructs were made by PCR amplification of the last 500 bp of the *HSL1* coding sequence using primers MSO593 (5′-TCC/CCC/GGG/CGA/TTA/AAG/TTA/CGA/AGG/ATA/CCG-3′) and MSO594 (5′-TGC/TCT/AGA/TGA/ACG/TCC/GGC/ATT/TCG/AAT/TAC-3′). The PCR product was digested with *Sma*I and *Xba*I (underlined) and ligated to YIplac211 or YIplac204 (23) containing three copies of the HA epitope inserted at the *Sal*I and *Hin*dIII sites (YIplac211-*HA* and YIplac204-*HA*). These vectors were cut with *Eco*RI, blunted with Klenow, and then cut with *Xba*I. *HSL1-HA*-YIplac211 was linearized with *Eco*RI and integrated into the *HSL1* locus of YJB11 by the one-step gene replacement technique to generate YJB90. Proper integration into the *HSL1* locus was verified by PCR. The *GAL-HSL1-HA*-YIplac204 plasmid containing the full-length *HSL1* gene was made by first replacing the *HSL1* promoter with the *GAL1-10* promoter in the *HSL1* locus using *GAL-5′-HSL1*-YIplac204. This plasmid was constructed by subcloning the first 500 bp of the *HSL1* coding sequence generated by PCR with primers MSO599 (5′-CGC/GGA/TCC/ATG/ACT/GGT/CAC/GTT/TCA/AAA/ACG/AGC-3′) and MSO600 (5′-CCC/AAG/CTT/ACG/TTT/GTG/TGA/GAT/ATC/AAT/TTC-3′) into the *Bam*HI and *Hin*dIII sites of YIplac204-*GAL*. The construct was linearized by cutting with *Xmn*I and integrated into the *HSL1* locus of a haploid yeast strain that had been transformed with *HSL1-HA*-YIplac211 (see above). The *GAL-HSL1-HA*-YIplac204 plasmid was then rescued from the *HSL1* locus by cutting total genomic DNA within the Amp^r gene by using the unique *Sca*I site, recircularizing, and transforming into *Escherichia coli*. The resulting *GAL-HSL1-HA*-YIplac204 plasmid was then linearized by cutting within the *TRP1* gene using *Ava*I for integration. *GAL-HSL1-HA*-pRS303 was constructed by cutting *GAL-HSL1-HA*-YIplac204 with *Hin*dIII, filling the resulting overhang with Klenow, and cutting with *Bam*HI to liberate *HSL1-HA*. This fragment was ligated to *GAL*-pRS303 that had been cut with *Xba*I, filled in with Klenow, and then cut with *Bam*HI. The *GAL-HSL1-HA*-pRS303 plasmid was cut with *Nhe*I for integration into the *HIS3* locus. *GAL-HSL1-HA*-YIplac128 was constructed by isolating the full-length *HSL1-HA* sequence from *GAL-HSL1-HA*-YIplac204 by cutting with *Bam*HI and *Hin*dIII and ligating to *GAL*-YIplac128 cut with the same enzymes. $GAL\text{-}HSL1^{\Delta kinase}\text{-}HA$-YIplac128 was constructed by PCR amplification of nucleotides 1453 to 2332 of *HSL1* using oligonucleotides MSO740 (5′-CCC/GGA/TCC/**ATG**/GAA/CCT/AGG/ATT/GAA/TAC/GC-3′) and MSO741 (5′-CGC/GGG/CCC/TCA/TTT/TCC/TTA/TTT/GTA/GAC/ACC/CC-3′), cut with *Bam*HI and *Apa*I, and subcloned into *GAL-HSL1-HA*-YIplac128 cut with the same enzymes, resulting in the removal of the sequence encoding the first 483 amino acids of Hsl1p and the addition of a start methionine (bold). $GAL\text{-}HSL1^{K110A}\text{-}HA$ was constructed by cutting $HSL1^{K110A}$-pACTII with *Bsa*AI and *Avr*II, isolating the resulting 1.4-kb fragment encoding the K110A mutation, and subcloning into *GAL-HSL1-HA*-YIplac128 to replace the wild-type sequence with the mutant one. $GAL\text{-}HSL1^{db\text{-}mut}\text{-}HA$-YIplac128 was created by Quikchange (Stratagene) mutagenesis of *GAL-HSL1-HA*-YIplac128 using MSO820 (5′-GGA/AGA/ACA/GAA/GCC/AAA/GGC/AGC/GGC/CGC/TTC/AGA/TAT/CAC/GGC/CTC/ATT/CAA/TAA/AAT/GAA/TAA/ACA/GG-3′) and MSO819 (5′-CCT/GTT/TAT/TCA/TTT/TAT/TGA/ATG/AGG/CCG/TGA/TAT/CTG/AAG/CGG/CCG/CTG/CCT/TTG/GCT/TCT/GTT/CTT/C-3′) as specified by the manufacturer; underlined residues correspond to nucleotide changes.

GAL-GIN4-HA was obtained by PCR amplification of full-length *GIN4* using MSO831 (5′-CCC/CCC/GGG/ATG/GCA/ATC/AAT/GGT/AAC/AGT/ATT/CCT/GCC-3′) and MSO832 (5′-CCC/GTC/GAC/TTT/TTG/TAG/AAC/GCC/TTC/CTT/ATT/CAG/G-3′), cut with *Sma*I and *Sal*I, ligated to *GAL*-YIplac128-*HA* cut with *Bam*HI, filled, and then cut with *Sal*I. *GAL-KCC4-HA*-YIplac128 was constructed in an analogous fashion using MSO833 (5′-CCC/CCC/GGG/ATG/ACT/GTG/GCG/AAT/ACC/GAG/ACC/C-3′) and MSO834 (5′-CCC/GTC/GAC/TTT/GTC/CAA/AAC/ACC/TTC/TTT/TTG-3′) to amplify the *KCC4* gene by PCR.

To disrupt *HSL1*, an *hsl1*Δ-YIplac204 disruption cassette was made. A 500-bp PCR fragment corresponding to the 5′ noncoding sequence just upstream of the *HSL1* gene coding region was generated using primers MSO665 (5′-CCC/GGA/TCC/GTC/ATT/TTC/GCG/TTG/GGT/TGT/TTG/GGC-3′) and MSO666 (5′-CCC/AAG/CTT/CGC/GAT/TAG/TAG/CAA/GTA/GTA/TGA/TGG-3′). The last 500 bp of the coding sequence was amplified by PCR using MSO667 (5′-CCC/GAA/TTC/AAC/AAG/AAT/AGT/ATC/GAC/TAT/C-3′) and MSO668 (5′-CCC/GGA/TCC/TGA/ACG/TCC/GGC/ATT/TCG/AAT/TAC-3′), digested with *Eco*RI and *Bam*HI, and then ligated to the YIplac204 vector cut with these enzymes to generate 3′-*HSL1*-YIplac204. The 5′-noncoding PCR product was digested with *Bam*HI and *Hin*dIII and ligated to 3′-*HSL1*-YIplac204 cut with the same enzymes to yield the *hsl1*Δ-YIplac204 disruption cassette. This construct was then digested with *Bam*HI and integrated into the *HSL1* locus. The P_{HSL1}-*HSL1-HA*-YIplac128 construct was made by PCR amplification of the 450-bp P_{HSL1} from pYB123 with oligonucleotides MSO704 (5′-CCC/GAA/TTC/GCG/TTG/GGT/TGT/TTG/GGC/TAA/ATA/GTG-3′) and MSO705 (5′-CCC/GGA/TTC/GTC/GTG/TGG/TAA/AAA/TAA/AAA/ATA/TTA/ATA/ACA/AAT/

TABLE 1. Yeast strains used in this study

Strain	Genotype	Source or reference
A991	*MAT***a** *bar1*Δ *cdc20-1*	75
JC310	*MAT***a** *cdc28-13* 3X (*GAL-CDC5-3XMYC:: URA3*)	9
JC311	*MAT***a** *cdc28-13* 3X (*GAL-CDC5-3XMYC:: URA3*) *cdh1*Δ*1::LEU2*	9
K3413	*MAT***a** *cln1,2,3*Δ*::LEU2 MET3-CLN2::TRP1 ade2-1 ade3-22 his3-11,15 ura3-1*	2
MaV103	*MAT***a** *SPAL10::URA3 leu2-3,112 trp1-901 his3*Δ*200 ade2-101 gal4*Δ *gal80*Δ *can1*^{r} *cyh2*^{r} *GAL1::HIS3@LYS2 GAL1::lacZ@URA3*	74
YJB10	K3413 *MAT*α	This study
YJB11	K3413 *MAT***a**/α	This study
YJB14	*MAT***a** *bar1*Δ	This study
YJB86	MaV103 [*CDH1*-pAS2]	This study
YJB87	MaV103 [*CDC20*-pAS2]	This study
YJB90	YJB11 *HSL-HA::URA3*	This study
YJB97	MaV103 [*CDC20*-pAS2 *MAD2*-pACT]	This study
YJB101	MaV103 [*CDC20*-pAS2 *HSL1*$^{\Delta kinase}$-pACT]	This study
YJB102	MaV103 [*CDC20*-pAS2 *HSL1*-pACTII]	This study
YJB103	MaV103 [*CDC20*-pAS2 *HSL1*^{K110A}-pACTII]	This study
YJB104	MaV103 [*CDC20*-pAS2 *SNF4*-pACT]	This study
YJB105	MaV103 [*CDH1*-pAS2 *HSL1*$^{\Delta kinase}$-pACT]	This study
YJB106	MaV103 [*CDH1*-pAS2 *HSL1*-pACTII]	This study
YJB107	MaV103 [*CDH1*-pAS2 *HSL1*^{K110A}-pACTII]	This study
YJB108	MaV103 [*CDH1*-pAS2 *SNF4*-pACT]	This study
YJB115	*MAT***a** *bar1*Δ *cdc23-1::URA3*	This study
YJB121	*MAT***a** *bar1*Δ *hsl1*Δ*::TRP1*	This study
YJB123	*MAT***a** *bar1*Δ *GAL-HSL1-HA::TRP1*	This study
YJB124	*MAT***a** *bar1*Δ *cdc20-1 GAL-HSL1-HA::TRP1*	This study
YJB125	*MAT***a** *bar1*Δ*::URA3 cdc23-1 GAL-HSL1-HA::TRP1*	This study
YJB131	*MAT***a**/α *HSL1*/*hsl1*Δ*::TRP1 CDC23*/*cdc23-1*	This study
YJB133	*MAT*α *hsl1*Δ*::TRP1*	This study
YJB156	YJB123 [*CDC20*-pEG-KT]	This study
YJB157	YJB123 [pEG-KT]	This study
YJB165	*MAT***a** *bar1*Δ *cdc28-13::URA3*	This study
YJB168	*MAT***a** *bar1*Δ *hsl1*Δ*::TRP1 HSL1-HA::LEU2*	This study
YJB172	*MAT***a**/α *HSL1*/*hsl1*Δ*::TRP1 CDC23*/*cdc23-1 SWE1*/*swe1*Δ*::LEU2*	This study
YJB177	*MAT***a**/α *HSL1*/*hsl1*Δ*::TRP1 CDC28*/*cdc28-13::URA3*	This study
YJB178	*MAT***a** *bar1*Δ *GAL-HSL1*$^{\Delta kinase}$*-HA::LEU2*	This study
YJB184	*MAT***a** *bar1*Δ *GAL-HSL1*^{K110A}*-HA::LEU2*	This study
YJB185	*MAT***a** *bar1*Δ *cdc20-1 GAL-HSL1*$^{\Delta kinase}$*-HA::LEU2*	This study
YJB189	*MAT***a** *bar1*Δ *GAL-HSL1-HA: TRP1 swe1*Δ*::URA3*	This study
YJB190	*MAT***a** *bar1*Δ *GAL-HSL1*^{K110A}*-HA::LEU2 swe1*Δ*::URA3*	This study
YJB191	*MAT***a** *bar1*Δ *GAL-HSL1*$^{\Delta kinase}$*-HA::LEU2 swe1*Δ*::URA3*	This study
YJB197	*MAT***a**/α *HSL1*/*hsl1*Δ*::TRP1 CDC28*/*cdc28-13::URA3 SWE1*/*swe1*Δ*::LEU2*	This study
YJB198	JC310 *GAL-HSL1-HA::HIS3*	This study
YJB199	JC311 *GAL-HSL1-HA::HIS3*	This study
YJB218	YJB123 [*CDH1*-pEG-KT]	This study
YJB221	YJB14 [*CDC20*-pEG-KT]	This study
YJB222	YJB14 [*CDH1*-pEG-KT]	This study
YJB223	YJB178 [*CDC20*-pEG-KT]	This study
YJB224	YJB178 [*CDH1*-pEG-KT]	This study
YJB225	YJB184 [*CDC20*-pEG-KT]	This study
YJB226	YJB184 [*CDH1*-pEG-KT]	This study
YJB229	*MAT***a** *bar1*Δ *GAL-HSL1*$^{db\text{-}mut}$*-HA::LEU2*	This study
YJB230	YJB229 [*CDC20*-pEG-KT]	This study
YJB231	YJB229 [*CDH1*-pEG-KT]	This study
YJB247	*MAT***a** *bar1*Δ *GAL-GIN4-HA::LEU2*	This study
YJB248	*MAT***a** *bar1*Δ *GAL-KCC4-HA::LEU2*	This study

AAA/GGA/GTG-3′) and subcloning into the *Eco*RI and *Bam*HI sites of YIplac128. The full-length *HSL-HA* was then subcloned into the *Bam*HI and *Hin*dIII sites of this construct. This plasmid was cut with *Afl*II for integration into the *LEU2* locus.

To disrupt *SWE1*, *swe1*Δ-YIplac128 and *swe1*Δ-YIplac211 disruption cassettes were made. The 5′ noncoding region of *SWE1* was amplified by PCR with primers MSO706 (5′-CCC/GTC/GAC/GGT/TCC/ACC/TCA/CAG/ATG/CC-3′) and MSO707 (5′-CCC/GGA/TCC/CTG/TTC/TCG/TGT/GCG/CCT/GTG-3′) and ligated into the *Bam*HI and *Sal*I sites of YIplac128 or YIplac211. The 3′-coding sequence of *SWE1* was amplified with primers MSO708 (5′-CCC/AAG/CTT/GCA/GCG/AAC/GTT/GTG/TTA/CC-3′) and MSO709 (5′-CCC/GTC/GAC/GGT/CCA/AAG/TCG/TCT/TCC/TGG-3′) and cloned into the *Hin*dIII and *Sal*I sites of either YIplac128 or YIplac211 containing the 5′ noncoding region of *SWE1*. The resulting disruption cassettes were then cut with *Sal*I and transformed into the appropriate yeast strains to replace *SWE1* with either *LEU2* or *URA3*, respectively.

To make the glutathione *S*-transferase (GST)-Cdc20p fusion protein in yeast, pEG-[KT]-*CDC20* was constructed by insertion of the full-length *CDC20* gene from *CDC20*-pAS2 into the *Sma*I and *Sal*I sites of pEG-[KT] (51). For the GST-Cdh1p fusion protein pEG-[KT]-*CDH1* was constructed by PCR amplification of the *CDH1* gene using primers MSO800 (5′-CCC/GGT/ACC/TCT/AGA/CAT/GTC/CAC/AAA/CCT/GAA/CCC-3′) and MSO801 (5′-CCC/GTC/GAC/ACG/TAT/TTG/ATT/AAA/TGC/GTC-3′) and subcloning into the *Xba*I and *Sal*I sites of the pEG-[KT] vector.

Library screening and β-galactosidase assays. Yeast two-hybrid screening was performed essentially as described previously (17). YJB87 was transformed with

the yeast two-hybrid library, and approximately 3.5×10^6 leucine prototrophs were analyzed for histidine prototrophy on plates containing 25 mM 3-amino-1,2,4-triazole (Sigma) and for β-galactosidase activity using a colony filter lift assay (8). For transformants yielding reproducibly high levels of β-galactosidase activity, loss of the *CDC20*-pAS2 bait plasmid was induced by growth in medium containing both tryptophan and cycloheximide (2.5 mg/ml; Sigma) and lacking leucine (27). Library plasmids were isolated from transformants that were blue only in the presence of the *CDC20*-pAS2 bait and not in the absence of a bait protein or in the presence of the *SNF1*-pAS2 bait (27). Plasmids were recovered in *E. coli*, subjected to sequencing, and confirmed to be in frame with the *GAL4* activation domain coding sequence. Levels of β-galactosidase activity were quantitated in a liquid assay using *o*-nitrophenyl-β-D-galactoside (ONPG) as described previously (25). All assays were done in triplicate.

Cell synchronizations and arrests. For the G_1 arrest and release experiment examining Hsl1p-HA expression, strain YJB90 was grown to an optical density at 600 nm (OD_{600}) of 0.2 in methionine-free medium at 30°C and arrested in G_1 by the addition of 1 mM methionine for 2.5 h. To release cells from the G_1 arrest, the cells were filtered, washed, resuspended in an equivalent volume of methionine-free medium, and grown at 30°C.

For Hsl1p-HA half-life experiments, cells of strains YJB123, YJB124, and YJB125 were grown in yeast peptone (YP) raffinose medium at 23°C to and OD_{600} of 0.35. The cells were then arrested in G_1 by the addition of α-factor (100 ng/ml; Sigma) for 2.5 h at 23°C. Hsl1p-HA expression was induced by the addition of galactose to 2% to the medium and incubation at 23°C for 1.5 h. Cells were shifted to 37°C for 1 h to inactivate *cdc20-1* and *cdc23-1*. Glucose (2%) and cycloheximide (1 mg/ml; Sigma) were added to terminate Hsl1p-HA synthesis, and incubation was continued at 37°C. For Hsl1p-HA half-life experiments with strains YJB198 and YJB199, cells were grown to an OD_{600} of 0.35 in YP raffinose medium. The cells were then shifted to 37°C to arrest them in G_1 by inactivation of *cdc28-13*. After 1 h at 37°C, 2% galactose was added to the medium to induce Hsl1p-HA expression and incubation was continued for 2 h at 37°C before glucose and cycloheximide were added. Experiments comparing the half-lives of Hsl1p-HA and $Hsl1p^{db\text{-}mut}$-HA in strains YJB123 and YJB229 were performed as described above, except that the cells were incubated at 30°C throughout the experiment. Samples for all experiments described above were processed for immunoblotting and fluorescence-activated cell sorter (FACS) analysis (see below).

Extract preparation and immunoblotting. For protein extracts, samples were subjected to bead beating four times for 1 min each in 10 mM Tris-HCl (pH 7.5)–10 mM NaN_3 (containing 10 μg each of leupeptin, chymostatin, and pepstatin per ml [Chemicon]) and centrifuged in a microcentrifuge for 5 min, and then the cell pellet was resuspended in 1× sample buffer (SB; 16.6% SDS, 26% glycerol, 262 mM Tris, 150 mM DTT), vortexed for 3 min, and boiled for 10 min. Extracts were centrifuged in a microcentrifuge for 5 min, and then the supernatant was centrifuged in a Beckman Optima ultracentrifuge at 70,000 rpm in the TLA-100.2 rotor for 10 min at 15°C.

Proteins were separated by sodium dodecyl sulfate (SDS)-polyacrylamide gel electrophoresis and transferred onto Immobilon-P membranes (Millipore). Membranes were blocked for 1 h in TBST BLOTTO (20 mM Tris-HCl [pH 7.5], 150 mM NaCl, 0.1% Tween, 5% milk) and then incubated overnight in TBST BLOTTO with affinity-purified polyclonal anti-HA antibodies (50 ng/ml; Santa Cruz Biotechnology) at 4°C. The blots were washed three times for 5 min each in TBST BLOTTO and then incubated in TBST BLOTTO with mouse anti-rabbit bridge antibody (0.2 μg/ml; Pierce) for 1 h at room temperature. The blots were then washed as above and incubated with appropriate antibodies coupled to horseradish peroxidase at 0.16 μg/ml (Pierce) for 1 h in TBST BLOTTO. The blots were then washed once in TBST BLOTTO, once in TBST, and once in TBS for 5 min each. Proteins were detected by chemiluminescence (SuperSignal; Pierce). Equal amounts of proteins were loaded in each lane. Total protein concentrations were determined using the Bio-Rad protein assay reagent.

Coimmunoprecipitation. For coexpression of Hsl1p-HA with GST-Cdc20p, GST-Cdh1p, or GST, strains YJB156, YJB218, and YJB157, respectively, were grown overnight in 5 ml of CM-Ura dextrose medium. These cells were then used to inoculate 100 ml of CM-Ura raffinose medium and grown overnight to an OD_{600} of 0.4. Galactose (4%) was added, and all cells were grown for 6 h to induce Hsl1p-HA and either GST-Cdc20p, GST-Cdh1p, or GST expression. Strains coexpressing $Hsl1p^{K110A}$-HA, $Hsl1p^{\Delta kinase}$-HA, or $Hsl1p^{db\text{-}mut}$-HA with either GST-Cdc20p or GST-Cdh1p (YJB225, YJB226, YJB223, YJB224, YJB230, and YJB231, respectively), as well as strains lacking an HA tag but containing GST-Cdc20p or GST-Cdh1p (YJB221 and YJB222), were induced in the same fashion. Cells were pelleted, frozen in liquid nitrogen, and stored at −80°C for future use. Cell pellets were thawed on ice and resuspended in 4 ml of IP buffer (50 mM potassium HEPES [pH 7.6], 1 mM EGTA, 1 mM $MgCl_2$. 0.1% Tween 20, 10% glycerol, 10 μg each of leupeptin, chymostatin, and pepstatin per ml). Cells were bead beaten with 0.6 g of glass beads eight times for 1 min with 2-min rests on ice between bursts (Mini-Beadbeater 8; BioSpec Products). Lysates were incubated on ice for an additional 15 min and centrifuged in a microcentrifuge for 10 min at 4°C. Samples were then diluted twofold with IP buffer and incubated for 1.5 h with 5 μg of affinity-purified anti-HA antibodies (Santa Cruz Biotechnology) at 4°C. Then 100 μl of protein A-agarose beads (50% slurry; Gibco/BRL) was washed in IP buffer and added to the extracts, which were incubated for an additional 1.5 h at 4°C. The beads were then gently pelleted and washed three times with 5 ml of IP buffer. Then 25 μl of beads was resuspended in 1× SB, separated by SDS-polyacrylamide gel electrophoresis and subjected to immunoblot analysis as described above using affinity-purified rabbit anti-GST antibodies. The blots were then stripped using 62.5 mM Tris-HCl (pH 6.7)–100 mM β-mercaptoethanol–2% SDS, washed with TBST, and reprobed with anti-HA antibodies.

TABLE 2. Yeast two-hybrid interactions[a]

AD fusion	β-Galactosidase activity (Miller units) for interaction with DB fusion[b]:	
	Cdc20p	Cdh1p
$Hsl1p^{\Delta kinase}$	66.4	21.0
Hsl1p	9.0	9.0
$HSL1p^{K110A}$	<0.1	4.0
Mad2p	59.5	ND[c]
Snf4p	<0.1	<0.1

[a] β-Galactosidase activity for interactions between Cdc20p or Cdh1p DNA-binding domain (DB) fusions with the listed Gal4 activation domain (AD) fusion proteins.

[b] Each numerical value represents the mean of three independent experiments.

[c] ND, not determined.

Other methods. To prepare cells for flow cytometry, 2 ml of cell culture for each time point was gently sonicated, pelleted, resuspended in an equal volume of 70% ethanol, and incubated for at least 2 h at room temperature. The cells were pelleted, washed twice with 50 mM Tris-HCl (pH 7.8), resuspended in 0.8 ml of the same buffer containing 250 μg of RNase A per ml, and incubated overnight at 37°C with rotation. The cells were pelleted, resuspended in 0.5 ml of 55 mM HCl containing 5 mg of pepsin (Boehringer Mannheim) per ml, and incubated for 30 min at 37°C. They were then washed once with 1 ml of 200 mM Tris-HCl (pH 7.5)–211 mM NaCl–78 mM $MgCl_2$ and resuspended in 0.5 ml of the same buffer containing 110 μg of propidium iodide (Sigma) per ml. Stained cells were analyzed by flow cytometry, using a previously described procedure (12), with a FACS Vantage flow cytometer (Becton-Dickinson, San Jose, Calif.). Cell cycle analysis was performed using the Modfit 5.2 model (Verity Software House).

Cells were fixed for light microscopy by adding 37% formaldehyde directly to the medium to a final concentration of 5% and incubating for 1 h at room temperature with gentle shaking. The cells were washed with 1× phosphate-buffered saline, mounted on glass slides, and viewed by Nomarski optics using a Zeiss microscope.

RESULTS

Cdc20p and Cdh1p interact with Hsl1p. Cdc20p has been shown previously to be involved in APC activation and is required to target Pds1p and the mitotic cyclin Clb5p for ubiquitination by the APC (5, 20, 53, 61). We set out to identify other APC substrates by using Cdc20p as the bait protein in a yeast two-hybrid screen. A yeast strain containing Cdc20p fused to the DNA-binding domain of Gal4p (Cdc20p-DB) was transformed with a yeast cDNA library encoding Gal4p activation domain fusion proteins (AD; a gift of Stephen Elledge). Approximately 3×10^6 transformants were analyzed for specific interaction with the Cdc20p bait protein. We isolated the genes encoding Mad1p (1 time), Mad2p (113 times), and Mad3p (8 times), which have been shown previously to interact with Cdc20p by this assay (30, 37). The binding of the Mad proteins to Cdc20p is believed to prevent Cdc20p from targeting Pds1p for ubiquitination by the APC, thereby preventing anaphase onset until all of the chromosomes are properly attached to the mitotic spindle (5, 20, 53).

We also detected a novel interaction between Cdc20p and Hsl1p (Table 2). Hsl1p is a 170-kDa protein that negatively regulates Swe1p (4, 48), a kinase that phosphorylates Cdc28p on Tyr-19 in a bud morphogenesis checkpoint (45, 62). The Hsl1p-AD fusion identified in this screen represents a truncated form of Hsl1p in which the amino-terminal 470 amino acids forming the kinase domain are absent ($Hsl1p^{\Delta kinase}$).

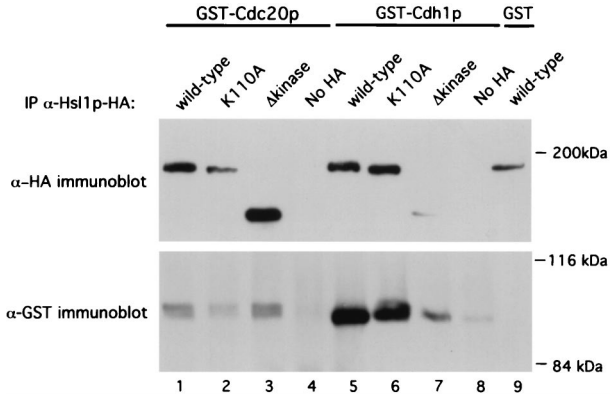

FIG. 1. Cdc20p and Cdh1p associate with Hsl1p in cell extracts. Extracts from yeast cells overexpressing Hsl1p-HA, Hsl1p^{K110A}-HA, or Hsl1p$^{\Delta kinase}$-HA with either GST-Cdc20p, GST-Cdh1p, or GST were incubated with anti-HA antibodies (Santa Cruz Biotechnology) to immunoprecipitate Hsl1p-HA, Hsl1p^{K110A}-HA, and Hsl1p$^{\Delta kinase}$-HA. Immunoprecipitates were separated by SDS-polyacrylamide gel electrophoresis and then immunoblotted with either anti-HA or anti-GST antibodies to detect different forms of Hsl1p-HA (upper panel) or coprecipitation of GST fusion proteins (lower panel). GST-Cdc20p and GST-Cdh1p specifically precipitated with Hsl1p-HA (lanes 1 and 5) and were not precipitated from extracts lacking an HA tag (lanes 4 and 8). Both GST-Cdc20p and GST-Cdh1p coprecipitated with Hsl1p$^{\Delta kinase}$-HA (lanes 3 and 7). No GST-immunoreactive band was detected in the strain expressing GST alone (lane 9). Lanes 1 to 9, strains YJB156, YJB225, YJB223, YJB221, YJB218, YJB226, YJB224, YJB222, and YJB157, respectively.

This protein interacted strongly with Cdc20p (Table 2). Full-length wild-type and catalytically inactive (Hsl1p^{K110A}) (4) forms of Hsl1p were constructed as Gal4p-AD fusions and tested for interaction with the Cdc20p-DB fusion. Full-length Hsl1p also interacted with Cdc20p, whereas interaction with the catalytically inactive form of Hsl1p was below the detection limit in this assay, similar to that of the Snf4p negative control (Table 2).

Yeast Cdh1p has significant sequence similarity to Cdc20p and also targets proteins for ubiquitination by the APC (9, 60, 75). We therefore tested the ability of the different Hsl1p-AD fusions to interact with a Cdh1p-DB fusion. Like Cdc20p, Cdh1p interacted with full-length Hsl1p and with the Hsl1p$^{\Delta kinase}$ fusion; however, Hsl1p^{K110A} also exhibited a detectable interaction with Cdh1p (Table 2). Cdh1p interaction with Mad2p was not tested in the liquid β-galactosidase assay; however, no interaction was detected in a filter lift assay (data not shown). These data suggest that both Cdc20p and Cdh1p can interact with Hsl1p in the yeast two-hybrid system. We do not know whether the quantitative differences in Table 2 reflect altered interactions or different expression levels of the various fusion proteins.

To further demonstrate an interaction between Hsl1p and Cdc20p or Cdh1p, coimmunoprecipitation studies were conducted. Constructs encoding HA-tagged wild-type (Hsl1p-HA), Hsl1p^{K110A}, and Hsl1p$^{\Delta kinase}$ proteins were made. Hsl1p-HA was shown to be fully functional by its ability to rescue the elongated bud phenotype of the *hsl1*Δ strain (see below). The different Hsl1p-HA constructs were coexpressed in a yeast strain with either GST-Cdc20p or GST-Cdh1p. Hsl1p-HA, Hsl1p^{K110A}-HA, and Hsl1p$^{\Delta kinase}$-HA were immunoprecipitated using antibodies against the HA tag, and the immunoprecipitates were analyzed for the presence of GST-Cdc20p or GST-Cdh1p by immunoblotting with antibodies directed against GST. Both GST-Cdc20p and GST-Cdh1p specifically coprecipitated with wild-type Hsl1p-HA (Fig. 1, lower panel, lanes 1 and 5). Similarly, both proteins were coprecipitated with Hsl1p$^{\Delta kinase}$-HA and Hsl1p^{K110A}-HA (lanes 2, 3, 6, and 7). The differences in the amounts of GST-Cdc20p and GST-Cdh1p in lanes 2 and 7 probably reflect the smaller amounts of Hsl1p proteins present in these immunoprecipitates. Only background amounts of GST-Cdc20p and GST-Cdh1p were precipitated with the anti-HA antibody in strains lacking an HA tag (lanes 4 and 8). No GST-immunoreactive band was detected when Hsl1p-HA was immunoprecipitated in a strain expressing GST alone (lane 9). These findings support the two-hybrid results and suggest that Hsl1p can associate either directly or indirectly with Cdc20p and Cdh1p in yeast cells.

Genetic interactions between *hsl1*Δ and *cdc23-1* are *SWE1* dependent. Genetic studies were conducted to gain insight into the nature of the Cdc20p-Hsl1p interaction, particularly into whether Hsl1p might regulate the APC. Although not essential for viability, cells lacking Hsl1p frequently have elongated buds due to increased Tyr-19 phosphorylation of Cdc28p by Swe1p, resulting in a defect in the switch from polarized to isotropic bud growth (4, 48) (see Fig. 3A). This phenotype can be suppressed by expressing a single copy of *HSL1-HA* from its own promoter, thus confirming that Hsl1p-HA is functional (see Fig. 3A and B).

We tested for genetic interactions between a strain with null mutation of *HSL1* (*hsl1*Δ) and a strain with a mutation in the APC by using *cdc23-1* mutant cells. Cdc23p is a core APC subunit, and the conditional mutation, *cdc23-1*, renders the APC inactive at the nonpermissive temperature of 37°C (31). *hsl1*Δ *cdc23-1* heterozygous diploids were constructed, and tetrad analysis was performed. If there were no genetic interaction between these two mutations, one would expect to obtain four viable spores at the permissive temperature of 23°C. In-

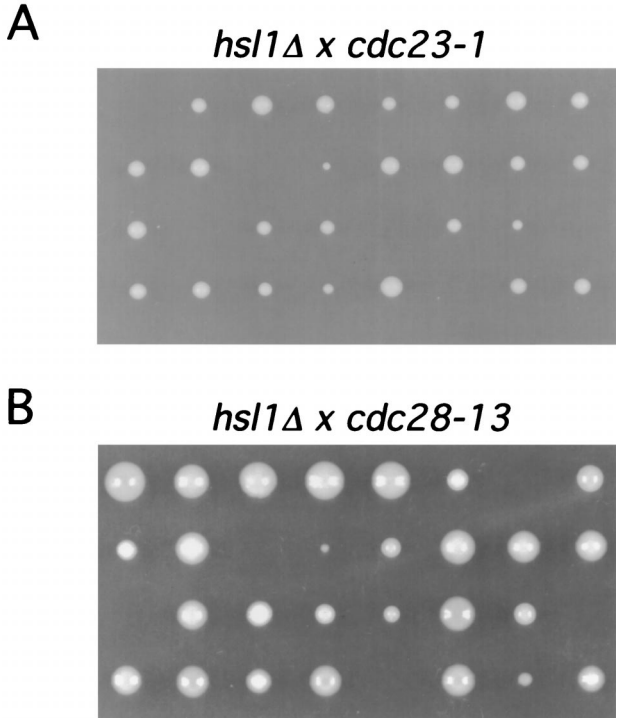

FIG. 2. Genetic interactions between *hsl1*Δ and *cdc23-1* and between *hsl1*Δ and *cdc28-13*. *hsl1*Δ*/HSL1 cdc23-1/CDC23* (YJB131) (A) and *hsl1*Δ*/HSL1 cdc28-13/CDC28* (YJB177) (B) heterozygous diploids were constructed and sporulated (see Materials and Methods). Tetrads were dissected, and the resulting spores were germinated at 23°C. The genotype of each colony was determined by plating onto selective media at 23 or 37°C.

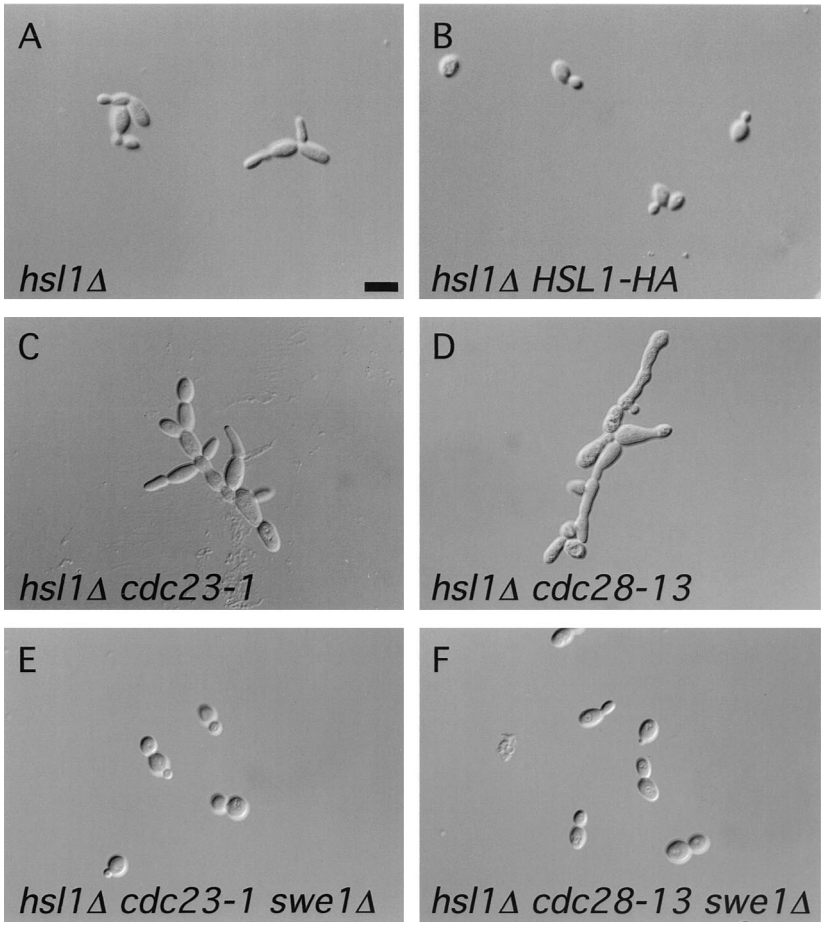

FIG. 3. Micrographs depicting cell morphologies of the indicated haploid strains. (A) Many *hsl1*Δ cells (strain YJB121) displayed elongated buds. (B) Normal bud morphology could be restored to *hsl1*Δ cells by a single copy of *HSL1-HA* (strain YJB168). (C) The *hsl1*Δ *cdc23-1* double mutant (derived from strain YJB131) had elongated buds and formed chains of cells. (D) *hsl1*Δ *cdc28-13* cells (progeny of strain YJB177) were extremely elongated, with an apparent cytokinesis defect. (E and F) Normal cell morphology of the *hsl1*Δ *cdc23-1* and *hsl1*Δ *cdc28-13* double mutants, respectively, was restored by deletion of *SWE1* (derived from strain YJB172 and YJB197, respectively). The cells depicted in panels A and B were grown at 30°C, whereas the cells in panels C to F were grown at 23°C. Bar, 4 μm.

stead, two, three, and four viable spores were observed in the tetrad dissections (Fig. 2A). In tetrads producing three viable spores, the genotype of the inviable spore was always determined to be *hsl1*Δ *cdc23-1*. Out of 96 spores analyzed, only 2 viable spores containing both mutations were isolated. Cells arising from these spore colonies showed poor growth at 23°C (data not shown). The cell morphology of these double mutants was abnormal, with cells forming long chains (Fig. 3C).

The genetic interaction between *hsl1*Δ and *cdc23-1* raised the possibility that Hsl1p directly activates the APC. However, another possibility was that Hsl1p indirectly activates the APC through inhibition of Swe1p, resulting in an increased level of active Cdc28p and consequent APC activation. To distinguish between these two possibilities, we tested whether the genetic interaction between *cdc23-1* and *hsl1*Δ was dependent on *SWE1*. We therefore made a diploid strain heterozygous for all three mutations (*hsl1*Δ *cdc23-1 swe1*Δ), sporulated the strain, and dissected the resulting tetrads. Genotype analysis of the resulting colonies identified many progeny containing all three mutations. These strains grew normally and no longer exhibited an abnormal cell morphology at 23°C (Fig. 3E). These results demonstrate that the synthetic interaction between *cdc23-1* and *hsl1*Δ was *SWE1* dependent and suggest that this genetic interaction is mediated through Cdc28p. We did not analyze genetic interactions between *hsl1*Δ and *cdc20-1* by tetrad analysis because we observed that *CDC20*/*cdc20-1* heterozygotes do not produce four viable spores at any temperature, suggesting that *CDC20* plays a role in some aspect of sporulation (data not shown). Tetrad analysis revealed no genetic interaction between *hsl1*Δ and *cdh1*Δ (data not shown).

We also observed a genetic interaction between *hsl1*Δ and *cdc28-13* by tetrad analysis of *hsl1*Δ *cdc28-13* heterozygous diploids (Fig. 2B). *cdc28-13* cells exhibit a G_1 arrest at the nonpermissive temperature due to a point mutation in the carboxyl terminus of the protein (47). Only four double mutants were isolated from the 48 spores whose genotypes were analyzed. These cells grew slowly and exhibited a *SWE1*-dependent elongated bud morphology (Fig. 3D and F and data not shown). These results, together with the *hsl1*Δ *cdc23-1* genetic interactions, suggest that Hsl1p regulates APC activity only indirectly by modulating Cdc28p-associated kinase activity through the inhibition of Swe1p and are consistent with previous results indicating a role for Cdc28p in APC activation (31). Consistent with Hsl1p not being a direct regulator of APC activity, we observed that overexpression of Hsl1p did not affect the timing of Pds1p degradation in synchronized cells (data not shown).

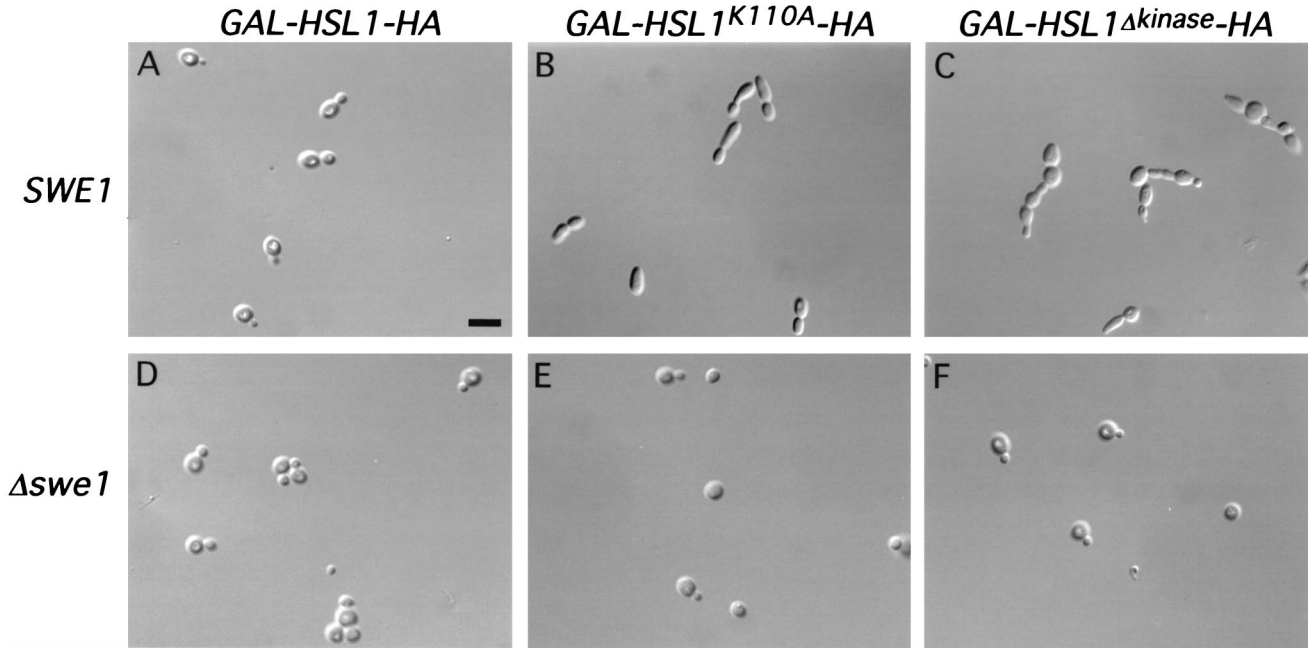

FIG. 4. Overexpression of catalytically inactive forms of *GAL-HSL1-HA* has dominant negative effects. Micrographs of cells overexpressing *GAL-HSL1-HA* (strain YJB123) and the catalytically inactive forms of *HSL1* (strains YJB184 and YJB178) in the presence of endogenous *HSL1* are shown. (A and B) Overexpression of *GAL-HSL1-HA* had no obvious effect on cell morphology, whereas cells overexpressing *GAL-HSL1*^{K110A}*-HA* had elongated buds. (C) Overexpression of *GAL-HSL1*$^{\Delta kinase}$*-HA* caused elongated buds and a cytokinesis defect. (D to F) Same strains as in panels A to C but with *SWE1* deleted (YJB189, YJB190 and YJB191). Bar, 4 μm.

Catalytically inactive forms of Hsl1p exert a dominant negative effect. We next tested the effect of overexpressing *HSL1*. *HSL1* was expressed from the *GAL1-10* promoter in wild-type, *cdc20-1*, and *cdc23-1* strains. We found no deleterious effects resulting from overproduction of wild-type *HSL1* in these strains (Fig. 4A and data not shown). However, overproduction of *HSL1*^{K110A} in wild-type cells resulted in an elongated-bud phenotype analogous to that of *hsl1*Δ cells (Fig. 3A), even though endogenous *HSL1* was present (Fig. 4B). Overexpression of *HSL1*$^{\Delta kinase}$ also caused elongated buds and an apparent cytokinesis defect, as seen by the formation of chains of cells (Fig. 4C). Both phenotypes were *SWE1* dependent, because a normal cell morphology was observed in these strains when *SWE1* was disrupted (Fig. 4E and F). The simplest interpretation of these results is that Hsl1p^{K110A} and Hsl1p$^{\Delta kinase}$ interfere with endogenous Hsl1p function. Phenotypic changes resulting from overexpression of the mutant forms of *HSL1* in *cdc20-1* and *cdc23-1* strains were less apparent for reasons that are currently unknown (data not shown).

Hsl1p degradation is APC dependent. The interaction between Hsl1p and Cdc20p and Cdh1p suggested that Hsl1p might be an APC substrate. To explore this possibility, the stability of Hsl1p-HA was examined during the cell cycle using synchronized cells. Cells from a strain lacking endogenous G_1 cyclins but containing *CLN2* behind the repressible *MET3* promoter (*cln1-3*Δ *MET3-CLN2*) can proliferate in the absence of methionine but arrest in G_1 in its presence due to repression of *CLN2* transcription (2). *HSL1* was HA tagged in this strain, and cells were arrested in G_1 and then released from the arrest by the addition to and then removal of methionine from medium. In the synchronized cells, Hsl1p was absent in G_1, appeared during S phase as the cells began to bud (45 min), was stable during mitosis, and rapidly disappeared at late anaphase (90 min) (Fig. 5). Hsl1p reappeared at 120 min as the cells began a new round of budding and cell division (Fig. 5). The absence of Hsl1p in G_1, when APC activity is high, and its presence during cell cycle stages when APC activity is low (S, G_2, and early M phases) is consistent with its being an APC substrate and is in agreement with a previous report regarding Hsl1p expression in synchronized cells (50).

To test whether Hsl1p is an APC substrate, the stability of Hsl1p-HA was investigated in wild-type and APC mutant cells (*cdc20-1* or *cdc23-1* mutant strains) arrested in G_1. Wild-type, *cdc20-1*, and *cdc23-1* strains containing *GAL-HSL1-HA* were arrested in G_1 with α-factor, induced to express Hsl1p-HA by growth in galactose, and then incubated at 37°C to inactivate *cdc20-1* and *cdc23-1*. At time zero, glucose and cycloheximide were added to terminate new synthesis of Hsl1p-HA. The level of Hsl1p was monitored by immunoblot analysis. Hsl1p-HA had a short half-life in wild-type cells, being undetectable within 30 min of glucose and cycloheximide addition (Fig. 6A, lanes 1 to 5). In contrast, Hsl1p was stable in *cdc23-1* mutant cells, with most of the protein still present after 60 min (lane 15). There was only minor stabilization of Hsl1p-HA in *cdc20-1* cells relative to the stabilization observed in *cdc23-1* cells (compare lanes 6 to 10 and lanes 11 to 15). FACS analysis confirmed that these cells remained arrested in G_1 (data not shown). Similar but slightly less efficient stabilization was observed for Hsl1p^{K110A}-HA and Hsl1p$^{\Delta kinase}$-HA in the *cdc23-1* strain (data not shown). These results indicate that Hsl1p is degraded in an APC-dependent manner.

Given that Hsl1p was found to interact with both Cdc20p and Cdh1p in the two-hybrid assay and by coprecipitation analysis (Table 2; Fig. 1), we next investigated whether deletion of *CDH1* resulted in stabilization of Hsl1p in G_1-arrested cells. Null mutants of *CDH1* are viable but unresponsive to α-factor due to elevated levels of Clb2p in these cells (60, 75). Cells were therefore arrested in G_1 using the temperature-

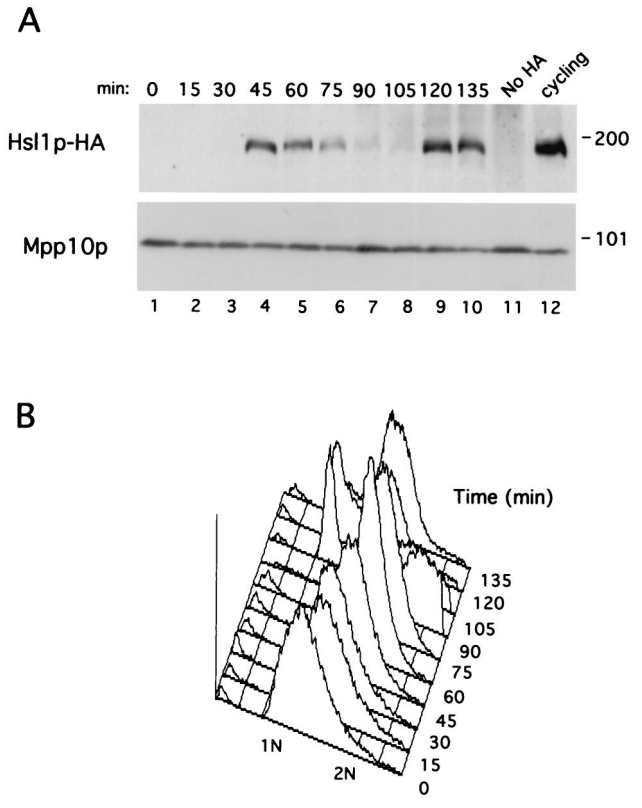

FIG. 5. Hsl1p-HA levels oscillate during the cell cycle in synchronized cells. Cells of yeast strain YJB90 (*cln1,2,3,Δ MET3-CLN2 HSL1-HA*) were arrested in G_1 by the addition of methionine to repress *CLN2* transcription. When the arrest was complete, a sample was taken for the zero time point and then cells were released from the arrest by resuspension in methionine-free medium. Samples were taken at the indicated times and processed for immunoblot analysis as described in Materials and Methods. (A) Immunoblot of Hsl1p-HA (upper panel) and Mpp10p (lower panel) during the G_1 arrest and release time course. Mpp10p is a nucleolar protein (16) whose levels are constant during the cell cycle. YJB90 cycling cells, molecular mass standards (in kilodaltons), and a strain lacking the HA epitope are shown at right. (B) FACS analysis of each time point to monitor the cell cycle position of the cells throughout the time course.

sensitive *cdc28-13* allele. *CDH1* or *cdh1*Δ cells containing *GAL-HSL1-HA* were shifted to 37°C and induced to express Hsl1p-HA by galactose addition. The stability of Hsl1p-HA was examined after termination of Hsl1p-HA synthesis as described above. Hsl1p-HA was stabilized in *cdh1*Δ cells, almost as much as was observed for *cdc23-1* cells (compare Fig. 6A, lane 15, with Fig. 6B, lane 10). These results suggest that Cdh1p is primarily responsible for the APC-mediated turnover of Hsl1p in G_1.

Hsl1p-related proteins are not APC substrates. Hsl1p has sequence homology to two other related protein kinases, Gin4p and Kcc4p, that colocalize with Hsl1p and the septins at the bud neck (4). Furthermore, like Hsl1p, these proteins have been proposed to negatively regulate Swe1p activity (4). We therefore wished to examine if Gin4p and Kcc4p were also regulated by APC-mediated protein turnover. *GAL-GIN4-HA* and *GAL-KCC4-HA* constructs were introduced into wild-type cells. Cells were arrested in G_1 with α-factor and induced to express Gin4p-HA and Kcc4p-HA by incubation in galactose. New Gin4p and Kcc4p synthesis was then inhibited by the addition of glucose and cycloheximide, and protein levels were monitored by immunoblot analysis using anti-HA antibodies. Unlike Hsl1p, both Gin4p and Kcc4p appear to be stable in G_1-arrested cells containing high levels of APC activity (Fig. 7). Furthermore, inactivation of the APC using *cdc23-1* cells did not result in an increased level or stability of these proteins (data not shown). These results indicate that neither Gin4p nor Kcc4p is degraded by the APC.

APC-mediated degradation of Hsl1p is destruction box dependent. APC substrates contain a 9-amino-acid destruction box motif with the consensus sequence RXXLXXXXN, where the arginine and leucine residues are the most highly conserved (24). We therefore wished to determine if the APC-dependent degradation of Hsl1p required an intact destruction box motif. Scanning Hsl1p reveals the sequence RAALSDITN, located after the kinase domain at amino acids 828 to 836. Since the arginine, leucine, and asparagine residues are most critical for destruction box function, we mutagenized these residues to alanine ($Hsl1p^{db\text{-}mut}$) (Fig. 8A) (see Materials and Methods). We then analyzed the stability of $Hsl1p^{db\text{-}mut}$ relative to wild-type Hsl1p in cells arrested in G_1. As described above, cells were arrested in G_1 with α-factor and induced to express the different forms of Hsl1p by galactose induction, and protein levels were monitored after glucose and cycloheximide addition to prevent new Hsl1p synthesis. $Hsl1p^{db\text{-}mut}$ was greatly stabilized relative to Hsl1p. In contrast to wild-type Hsl1p, which was virtually undetectable at the 30-min time point, $Hsl1p^{db\text{-}mut}$ was readily detectable at the 60-min time point (Fig. 8B, compare lanes 4 and 10). In agreement with these findings, we observed that $Hsl1p^{db\text{-}mut}$-HA expressed from the endogenous *HSL1* promoter was present throughout the cell cycle in synchronized cells (data not shown). These data indicate that Hsl1p degradation is largely destruction box dependent.

We next wished to investigate whether $Hsl1p^{db\text{-}mut}$ could associate with either Cdc20p or Cdh1p. As demonstrated in Fig. 1, wild-type Hsl1p-HA efficiently coimmunoprecipitated both GST-Cdc20p and GST-Cdh1p (Fig. 8C, lower panel, lanes 1 and 4). Interestingly, GST-Cdc20p was undetectable in $Hsl1p^{db\text{-}mut}$-HA immunoprecipitates (lane 2) and the efficiency of GST-Cdh1p coprecipitation was considerably reduced (compare lanes 4 and 5). Approximately equal amounts of Hsl1p-HA and $Hsl1p^{db\text{-}mut}$-HA were detectable in the anti-HA immunoprecipitates (Fig. 8C, upper panels, lanes 1 and 2 and lanes 4 and 5). These data suggest that the destruction box motif of Hsl1p is critical for association with Cdc20p and enhances its association with Cdh1p. Taken together, the above data strongly suggest that Hsl1p is an APC substrate.

DISCUSSION

Hsl1p is an APC substrate. Using Cdc20p, an APC activator protein, in a yeast two-hybrid screen, we have identified a novel interaction with the Hsl1p protein kinase. Evidence presented in this work suggests that Hsl1p is an APC substrate: (i) Hsl1p can associate with two APC subunits, Cdc20p and Cdh1p; (ii) Hsl1p levels oscillate during the cell cycle, being present when APC activity is low and absent when APC activity is high; (iii) Hsl1p is stabilized by mutations that compromise APC activity; and (iv) mutation of a destruction box sequence in Hsl1p leads to Hsl1p stabilization.

Hsl1p interacted with both Cdc20p and Cdh1p in the yeast two-hybrid assay and by coimmunoprecipitation in yeast extracts. The clone of *HSL1* initially identified in the two-hybrid screen encoded a truncated form of Hsl1p lacking its amino-terminal kinase domain ($Hsl1p^{\Delta kinase}$). Analysis of full-length Hsl1p by both two-hybrid analysis and coimmunoprecipitation studies revealed that it could also bind Cdc20p and Cdh1p. Cdh1p appeared to coimmunoprecipitate more efficiently with

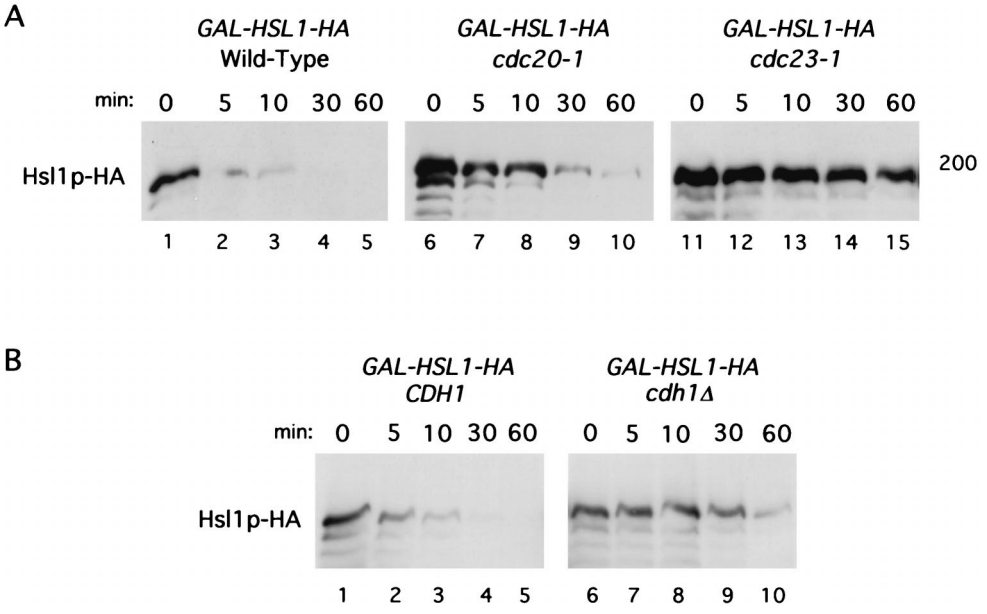

FIG. 6. Hsl1p-HA has a short half-life in G_1 and is stabilized by mutations that compromise APC activity. (A) Wild-type (strain YJB123), *cdc20-1* (strain YJB124), and *cdc23-1* (strain YJB125) strains containing an integrated copy of *GAL-HSL1-HA* were arrested in G_1 with α-factor, induced to express *GAL-HSL1-HA* by the addition of galactose for 1.5 h, and then shifted to 37°C for 1 h to inactivate *cdc20-1* or *cdc23-1*. The zero time point sample was taken, and then glucose and cycloheximide were added to terminate transcription and translation, respectively. Cell samples were taken at the indicated times and processed for immunoblot analysis as described in Materials and Methods. (B) YJB198 (*CDH1 cdc28-13*) or YJB199 (*cdh1Δ cdc28-13*) cells containing *GAL-HSL1-HA* were arrested in G_1 by shifting the cells to 37°C to inactivate *cdc28-13*. After 1 h at 37°C, cells were induced to express *GAL-HSL1-HA* by the addition of galactose and incubated for an additional 2 h at 37°C. A zero time point sample was taken, and then glucose and cycloheximide were added to terminate new synthesis of Hsl1p-HA. Cell samples were taken at the indicated times after glucose and cycloheximide addition. FACS analysis confirmed that cells remained arrested in G_1 at all time points in both panels A and B (data not shown).

the different forms of Hsl1p than did Cdc20p; however, this probably reflects the lower levels of Cdc20p in the cell. Cdc20p, but not Cdh1p, oscillates during the cell cycle and is short-lived (19, 59).

In agreement with the two-hybrid and coprecipitation findings, deletion of *CDH1*, encoding a WD40 domain protein involved in APC activation, resulted in Hsl1p stabilization during G_1, when *HSL1* was expressed from the *GAL1-10* promoter (Fig. 6). These results suggest that the purpose of the Hsl1p-Cdh1p interaction is to mediate Hsl1p ubiquitination and subsequent degradation. Consistent with this interpretation is the finding that a mutation in *CDC23*, encoding a core APC subunit, also results in Hsl1p stabilization in G_1.

The function of the Hsl1p-Cdc20p interaction is less obvious, since a mutation in *CDC20* had only a modest effect on Hsl1p stability in G_1 (Fig. 6A). One possibility is that Cdc20p is responsible for mediating Hsl1p degradation during late mitosis whereas Cdh1p plays this role during G_1. This has been reported to be the case for Clb3p, another APC substrate, and other mitotic cyclins (46, 53, 78). Alternatively, it is possible that Hsl1p is capable of interacting with Cdc20p based on its sequence conservation with Cdh1p, but only Cdh1p directs the degradation of Hsl1p. The third possibility, which cannot be excluded, is that Cdc20p interacts with Hsl1p for reasons independent of Hsl1p turnover.

In agreement with Hsl1p being an APC substrate, we observed that mutation of a destruction box motif within Hsl1p resulted in stabilization of this protein. Interestingly, this mutation also resulted in the disruption of the Hsl1p-Cdc20p interaction and reduced the interaction between Hsl1p and Cdh1p in coprecipitation analyses. These findings suggest that Cdc20p and, to a lesser extent, Cdh1p may target protein substrates for APC-mediated ubiquitination through recognition of the destruction box motif within the substrate. The stabilization of $Hsl1p^{db\text{-}mut}$ was not as complete as was observed for wild-type Hsl1p in a *cdc23-1* strain (Fig. 6A and 8B). A possible explanation for this result is the observation that Cdh1p is still capable of some interaction with the destruction box mutant of Hsl1p and may therefore still target $Hsl1p^{db\text{-}mut}$ for APC-mediated ubiquitination, albeit at a reduced efficiency. In agreement with this proposal, it was recently found that the ubiquitination of human cyclin B in vitro was strongly dependent on an intact destruction box for Cdc20p-activated APC, whereas Cdh1p-activated APC could still ubiquitinate the cyclin B destruction box mutant (19). It is also possible that Hsl1p has a weaker destruction box sequence, allowing for some degradation of $Hsl1p^{db\text{-}mut}$; however, we think that this is a less likely explanation, given that Cdc20p fails to interact with $Hsl1p^{db\text{-}mut}$.

Recently, human Cdc20p was found to associate with cyclin A by both two-hybrid analysis and in cell extracts by coprecipitation (55). Interestingly, the association between Cdc20p and

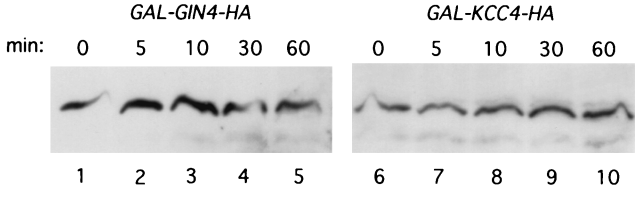

FIG. 7. Gin4p-HA and Kcc4p-HA are stable in G_1-arrested cells. Wild-type cells containing an integrated copy of *GAL-GIN4-HA* (strain YJB247) or *GAL-KCC4-HA* (strain YJB248) were arrested in G_1 with α-factor and induced to express either gene product by the addition of galactose to the medium for 2.5 h at 30°C. A zero time point sample was taken, and then glucose and cycloheximide were added to terminate new synthesis or Gin4p-HA or Kcc4p-HA. Samples were taken at the indicated time points after glucose and cycloheximide addition.

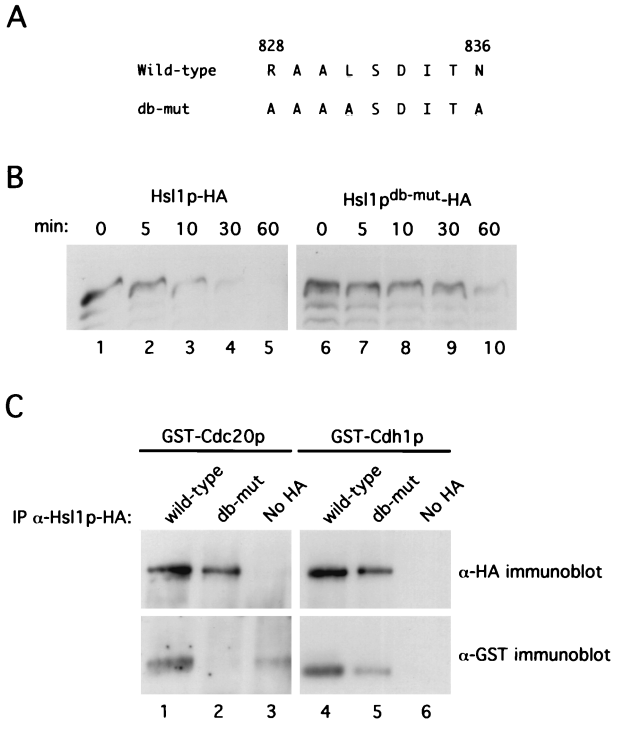

FIG. 8. Hsl1p-HA degradation and association with Cdc20p and Cdh1p are destruction box dependent. (A) Amino acid sequence of wild-type and Hsl1p$^{db\text{-}mut}$-HA proteins at residues 828 to 836. Underlined residues represent amino acid changes in the putative destruction box sequence. (B) Hsl1p$^{db\text{-}mut}$-HA is stabilized in G_1-arrested cells relative to wild-type Hsl1p-HA. Cells containing *GAL-HSL1-HA* (strain YJB123) or *GAL-HSL1$^{db\text{-}mut}$-HA* (strain YJB229) were arrested in G_1 with α-factor and induced to express the different forms of Hsl1p by addition of galactose to the medium for 2.5 h. A zero time point sample was taken, glucose and cycloheximide were added to terminate new synthesis of Hsl1p-HA and Hsl1p$^{db\text{-}mut}$-HA, and samples were taken at time points as indicated. (C) Hsl1p-HA but not Hsl1p$^{db\text{-}mut}$-HA can efficiently coimmunoprecipitate GST-Cdc20p and GST-Cdh1p. Hsl1p-HA and Hsl1p$^{db\text{-}mut}$-HA were immunoprecipitated (IP) from cell extracts coexpressing either GST-Cdc20p or GST-Cdh1p with anti-HA antibodies and then probed for the levels of Hsl1p-HA (upper panels) or GST-Cdc20p or GST-Cdh1p (lower panels) by immunoblot analysis with anti-HA or anti-GST antibodies, respectively.

cyclin A required a region between the destruction box and the cyclin box of cyclin A but mutation of the destruction box itself did not disrupt the interaction (55). The reason for this discrepancy with our present results is unclear. Perhaps Cdc20p recognizes different domains on different APC substrates. Alternatively, the domain they identified might represent a region of cyclin A required for Cdc20p binding during cyclin A-Cdk2-mediated phosphorylation of Cdc20p (55).

Although it seems likely that Hsl1p binds directly to Cdc20p and Cdh1p, it is possible that the interaction is indirect and occurs through another APC subunit (19, 42, 43, 79). The differential effect of Hsl1p$^{db\text{-}mut}$ on the associations with Cdc20p and Cdh1p suggests that the interaction occurs directly between these proteins rather than via a shared core APC subunit. Future work using recombinant proteins will be necessary to address whether Hsl11p and other APC substrates associate directly with Cdc20p and/or Cdh1p or indirectly through other APC subunits and which domains of the APC substrates are necessary and sufficient for association with the APC machinery.

Why is Hsl1p an APC substrate? Why Hsl1p is targeted for ubiquitin-mediated degradation by the APC during the cell cycle is unclear. It is tempting to speculate that the inactivation of Hsl1p by degradation in late mitosis is necessary to allow Swe1p to perform its role in the bud morphogenesis pathway in the G_1 and S phases of the subsequent cell cycle. However, we observed no apparent change in the expression pattern of Swe1p in cells expressing Hsl1p$^{db\text{-}mut}$ from the *HSL1* promoter relative to cells with wild-type Hsl1p (data not shown). Unlike wild-type Hsl1p, Hsl1p$^{db\text{-}mut}$ was expressed throughout the cell cycle, including G_1, although the levels of Hsl1p$^{db\text{-}mut}$ were clearly higher during mitosis (data not shown). *HSL1* mRNA levels vary during the cell cycle (68) and may in part account for this fluctuation. Furthermore, it is likely that Cdh1p can at least partially promote Hsl1p$^{db\text{-}mut}$ degradation, since it can still associate with Hsl1p$^{db\text{-}mut}$ (Fig. 8C). Therefore, complete Hsl1p degradation does not seem to be required for cell cycle progression in unperturbed cells. Recently, McMillan et al. demonstrated that overexpression of Hsl1p can override a G_2/M delay imposed by the morphogenic checkpoint (50). It will be of interest to investigate whether cells expressing Hsl1p$^{db\text{-}mut}$ can overcome a morphogenic checkpoint arrest resulting from improper bud formation.

The reason why Hsl1p is degraded in an APC-dependent fashion while the related kinases Gin4p and Kcc4p are not is presently unknown. All three kinases have been proposed to inhibit Swe1p, a kinase that inhibits Cdc28p in a bud morphogenesis checkpoint, and thus prevent the inhibition of Cdc28p when proper bud formation has occurred (4). It is conceivable that Hsl1p is the kinase that is primarily responsible for Swe1p inhibition in this pathway. In agreement with this idea, only Hsl1p has thus far been shown to promote Swe1p degradation by the SCF^{Met30} ubiquitin ligase (50). Alternatively, Gin4p or Kcc4p may function in some other aspect of the morphogenic checkpoint not related to Swe1p inhibition.

Results from this study have identified Hsl1p as a novel APC substrate. The role of Hsl1p in promoting degradation of Swe1p by SCF therefore suggests that Hsl1p can serve as a link between the APC and SCF pathways. Given that protein degradation is an irreversible process, it would not be surprising if extensive communication exists between the SCF and APC proteolytic systems to ensure the proper timing of degradation of key cell cycle regulators during cell cycle progression.

ACKNOWLEDGMENTS

We thank Angelika Amon, Yves Barral, Daniel Burke, Steve Elledge, David Morgan, and Zhaoxia Sun for providing yeast strains and plasmids. We thank Steve Elledge for the yeast two-hybrid library, Susan Baserga for the anti-Mpp10p antibodies, and Zachary Pitluk for affinity-purified anti-GST antibodies. We thank Rocco Carbone from The Yale Cancer Center Flow Cytometry Shared Resource (U.S. Public Health Service grant CA-16359) for performing FACS analysis. We thank Adrienne Natrillo for technical assistance and Aiyang Cheng, Philipp Kaldis, Karen Ross, and David Stern for critical reading of the manuscript. We thank Jonathan Raser, Daniel Lew, and Orna Cohen-Fix for insightful discussions.

This work was supported by a Jane Coffin Childs Fellowship awarded to J.L.B. and by grants 4512 from the Council for Tobacco Research and GM47830 from the NIH awarded to M.J.S.

REFERENCES

1. **Amon, A.** 1997. Regulation of B-type cyclin proteolysis by Cdc28-associated kinases in budding yeast. EMBO J. **16:**2693–2702.
2. **Amon, A., S. Irniger, and K. Nasmyth.** 1994. Closing the cell cycle circle in yeast: G2 cyclin proteolysis initiated at mitosis persists until the activation of G1 cyclins in the next cycle. Cell **77:**1037–1050.
3. **Amon, A., U. Surana, I. Muroff, and K. Nasmyth.** 1992. Regulation of p34^{CDC28} tyrosine phosphorylation is not required for entry into mitosis in *S. cerevisiae*. Nature **355:**368–371.
4. **Barral, Y., M. Parra, S. Bidlingmaier, and M. Snyder.** 1999. Nim1-related kinases coordinate cell cycle progression with the organization of the peripheral cytoskeleton in yeast. Genes Dev. **13:**176–187.

5. **Biggins, S., and A. W. Murray.** 1998. Sister chromatid cohesion in mitosis. Curr. Opin. Cell Biol. **10:**769–775.
6. **Booher, R. N., R. J. Deshaies, and M. W. Kirschner.** 1993. Properties of *Saccharomyces cerevisiae* wee1 and its differential regulation of $p34^{CDC28}$ in response to G_1 and G_2 cyclins. EMBO J. **12:**3417–3426.
7. **Brandeis, M., and T. Hunt.** 1996. The proteolysis of mitotic cyclins in mammalian cells persists from the end of mitosis until the onset of S phase. EMBO J. **15:**5280–5289.
8. **Breeden, L., and K. Nasmyth.** 1985. Regulation of the HO gene. Cold Spring Harbor Symp. Quant. Biol. **50:**643–650.
9. **Charles, J. F., S. L. Jaspersen, R. L. Tinker-Kulberg, L. Hwang, A. Szidon, and D. O. Morgan.** 1998. The Polo-related kinase Cdc5 activates and is destroyed by the mitotic cyclin destruction machinery in *S. cerevisiae*. Curr. Biol. **8:**497–507.
10. **Ciosk, R., W. Zachariae, C. Michaelis, A. Shevchenko, M. Mann, and K. Nasmyth.** 1998. An ESP1/PDS1 complex regulates loss of sister chromatid cohesion at the metaphase to anaphase transition in yeast. Cell **93:**1067–1076.
11. **Cohen-Fix, O., J. M. Peters, M. W. Kirschner, and D. Koshland.** 1996. Anaphase initiation in *Saccharomyces cerevisiae* is controlled by the APC-dependent degradation of the anaphase inhibitor Pds1p. Genes Dev. **10:**3081–3093.
12. **Crissman, H. A., and G. T. Hirons.** 1994. Staining of DNA in live and fixed cells. Methods Cell Biol. **41:**195–209.
13. **Cvrckova, F., and K. Nasmyth.** 1993. Yeast G_1 cyclins *CLN1* and *CLN2* and a GAP-like protein have a role in bud formation. EMBO J. **12:**5277–5286.
14. **Dawson, I. A., S. Roth, and S. Artavanis-Tsakonas.** 1995. The *Drosophila* cell cycle gene *fizzy* is required for normal degradation of cyclins A and B during mitosis and has homology to the *CDC20* gene of *Saccharomyces cerevisiae*. J. Cell Biol. **129:**725–737.
15. **Deshaies, R. J., V. Chau, and M. W. Kirschner.** 1995. Ubiquitination of the G_1 cyclin Cln2p by a Cdc34p-dependent pathway. EMBO J. **14:**303–312.
16. **Dunbar, D. A., S. Wormsley, T. M. Agentis, and S. J. Baserga.** 1997. Mpp10p, a U3 small nucleolar ribonucleoprotein component required for pre-18S rRNA processing in yeast. Mol. Cell. Biol. **17:**5803–5812.
17. **Durfee, T., K. Becherer, P. L. Chen, S. H. Yeh, Y. Yang, A. E. Kilburn, W. H. Lee, and S. J. Elledge.** 1993. The retinoblastoma protein associates with the protein phosphatase type 1 catalytic subunit. Genes Dev. **7:**555–569.
18. **Espinoza, F. H., A. Farrell, H. Erdjument-Bromage, P. Tempst, and D. O. Morgan.** 1996. A cyclin-dependent kinase-activating kinase (CAK) in budding yeast unrelated to vertebrate CAK. Science **273:**1714–1717.
19. **Fang, G., H. Yu, and M. W. Kirschner.** 1998. Direct binding of CDC20 protein family members activates the anaphase-promoting complex in mitosis and G1. Mol. Cell **2:**163–171.
20. **Farr, K. A., and O. Cohen-Fix.** 1999. The metaphase to anaphase transition: a case of productive destruction. Eur. J. Biochem. **263:**14–19.
21. **Feldman, R. M., C. C. Correll, K. B. Kaplan, and R. J. Deshaies.** 1997. A complex of Cdc4p, Skp1p, and Cdc53p/cullin catalyzes ubiquitination of the phosphorylated CDK inhibitor Sic1p. Cell **91:**221–230.
22. **Gietz, R. D., R. H. Schiestl, A. R. Willems, and R. A. Woods.** 1995. Studies on the transformation of intact yeast cells by the LiAc/SS-DNA/PEG procedure. Yeast **11:**355–360.
23. **Gietz, R. D., and A. Sugino.** 1988. New yeast-*Escherichia coli* shuttle vectors constructed with in vitro mutagenized yeast genes lacking six-base pair restriction sites. Gene **74:**527–534.
24. **Glotzer, M., A. W. Murray, and M. W. Kirschner.** 1991. Cyclin is degraded by the ubiquitin pathway. Nature **349:**132–138.
25. **Guarante, L.** 1983. Yeast promoters and *lacZ* fusions designed to study expression of cloned genes in yeast. Methods Enzmol. **101:**181–191.
26. **Guthrie, C., and G. R. Fink.** 1991. Guide to yeast genetics and molecular biology. Methods in enzymology, vol. 194. Academic Press, Inc., San Diego, Calif.
27. **Harper, J. W., G. R. Adami, N. Wei, K. Keyomarsi, and S. J. Elledge.** 1993. The p21 Cdk-interacting protein Cip1 is a potent inhibitor of G1 cyclin-dependent kinases. Cell **75:**805–816.
28. **Hochstrasser, M.** 1995. Ubiquitin, proteasomes, and the regulation of intracellular protein degradation. Curr. Opin. Cell Biol. **7:**215–223.
29. **Hochstrasser, M.** 1996. Ubiquitin-dependent protein degradation. Annu. Rev. Genet. **30:**405–439.
30. **Hwang, L. H., L. F. Lau, D. L. Smith, C. A. Mistrot, K. G. Hardwick, E. S. Hwang, A. Amon, and A. W. Murray.** 1998. Budding yeast Cdc20: a target of the spindle checkpoint. Science **279:**1041–1044.
31. **Irniger, S., S. Piatti, C. Michaelis, and K. Nasmyth.** 1995. Genes involved in sister chromatid separation are needed for B-type cyclin proteolysis in budding yeast. Cell **81:**269–278.
32. **Jaspersen, S. L., J. F. Charles, R. L. Tinker-Kulberg, and D. O. Morgan.** 1998. A late mitotic regulatory network controlling cyclin destruction in *Saccharomyces cerevisiae*. Mol. Biol. Cell **9:**2803–2817.
33. **Juang, Y. L., J. Huang, J. M. Peters, M. E. McLaughlin, C. Y. Tai, and D. Pellman.** 1997. APC-mediated proteolysis of Ase1 and the morphogenesis of the mitotic spindle. Science **275:**1311–1314.
34. **Kaiser, P., R. A. Sia, E. G. Bardes, D. J. Lew, and S. I. Reed.** 1998. Cdc34 and the F-box protein Met30 are required for degradation of the Cdk-inhibitory kinase Swe1. Genes Dev. **12:**2587–2597.
35. **Kaldis, P.** 1999. The cdk-activating kinase (CAK): from yeast to mammals. Cell. Mol. Life Sci. **55:**284–296.
36. **Kaldis, P., A. Sutton, and M. J. Solomon.** 1996. The Cdk-activating kinase (CAK) from budding yeast. Cell **86:**553–564.
37. **Kim, S. H., D. P. Lin, S. Matsumoto, A. Kitazono, and T. Matsumoto.** 1998. Fission yeast Slp1: an effector of the Mad2-dependent spindle checkpoint. Science **279:**1045–1047.
38. **King, R. W., R. J. Deshaies, J. M. Peters, and M. W. Kirschner.** 1996. How proteolysis drives the cell cycle. Science **274:**1652–1659.
39. **King, R. W., M. Glotzer, and M. W. Kirschner.** 1996. Mutagenic analysis of the destruction signal of mitotic cyclins and structural characterization of ubiquitinated intermediates. Mol. Biol. Cell **7:**1343–1357.
40. **King, R. W., P. K. Jackson, and M. W. Kirschner.** 1994. Mitosis in transition. Cell **79:**563–571.
41. **King, R. W., J. M. Peters, S. Tugendreich, M. Rolfe, P. Hieter, and M. W. Kirschner.** 1995. A 20S complex containing CDC27 and CDC16 catalyzes the mitosis-specific conjugation of ubiquitin to cyclin B. Cell **81:**279–288.
42. **Kotani, S., H. Tanaka, H. Yasuda, and K. Todokoro.** 1999. Regulation of APC activity by phosphorylation and regulatory factors. J. Cell Biol. **146:**791–800.
43. **Kramer, E. R., C. Gieffers, G. Holzl, M. Hengstschlager, and J. M. Peters.** 1998. Activation of the human anaphase-promoting complex by proteins of the CDC20/Fizzy family. Curr. Biol. **8:**1207–1210.
44. **Krek, W.** 1998. Proteolysis and the G1-S transition: the SCF connection. Curr. Opin. Genet. Dev. **8:**36–42.
45. **Lew, D. J., and S. I. Reed.** 1995. A cell cycle checkpoint monitors cell morphogenesis in budding yeast. J. Cell Biol. **129:**739–749.
46. **Lim, H. H., P.-Y. Goh, and U. Surana.** 1998. Cdc20 is essential for the cyclosome-mediated proteolysis of both Pds1 and Clb2 during M phase in budding yeast. Curr. Biol. **8:**231–234.
47. **Lörincz, A., and S. I. Reed.** 1986. Sequence analysis of temperature-sensitive mutations in the *Saccharomyces cerevisiae* gene *CDC28*. Mol. Cell. Biol. **6:**4099–4103.
48. **Ma, X. J., Q. Lu, and M. Grunstein.** 1996. A search for proteins that interact genetically with histone H3 and H4 amino termini uncovers novel regulators of the Swe1 kinase in *S. cerevisiae*. Genes Dev. **10:**1327–1340.
49. **McGarry, T. J., and M. W. Kirschner.** 1998. Geminin, an inhibitor of DNA replication is degraded during mitosis. Cell **93:**1043–1053.
50. **McMillan, J. N., M. S. Longtine, R. A. L. Sia, C. L. Theesfeld, E. S. G. Bardes, J. R. Pringle, and D. J. Lew.** 1999. The morphogenesis checkpoint in *Saccharomyces cerevisiae*: cell cycle control of Swe1p degradation by Hsl1p and Hsl7p. Mol. Cell. Biol. **19:**6929–6939.
51. **Mitchell, D. A., T. K. Marshall, and R. J. Deschenes.** 1993. Vectors for the inducible overexpression of glutathione S-transferase fusion proteins in yeast. Yeast **9:**715–722.
52. **Morgan, D. O.** 1995. Principles of Cdk regulation. Nature **374:**131–134.
53. **Morgan, D. O.** 1999. Regulation of the APC and the exit from mitosis. Nat. Cell Biol. **1:**E47–E53.
54. **Nasmyth, K.** 1993. Control of the yeast cell cycle by the Cdc28 protein kinase. Curr. Opin. Cell Biol. **5:**166–179.
55. **Ohtoshi, A., T. Maeda, H. Higashi, S. Ashizawa, and M. Hatakeyama.** 2000. Human p55/Cdc20 associates with cyclin A and is phosphorylated by the cyclin A-Cdk2 complex. Biochem. Biophys. Res. Commun. **268:**530–534.
56. **Patton, E. E., A. R. Willems, and M. Tyers.** 1998. Combinatorial control in ubiquitin-dependent proteolysis: don't Skp the F-box hypothesis. Trends Genet. **14:**236–243.
57. **Peters, J. M.** 1998. SCF and APC: the Yin and Yang of cell cycle regulated proteolysis. Curr. Opin. Cell Biol. **10:**759–768.
58. **Pines, J.** 1995. Cyclins and cyclin-dependent kinases: a biochemical view. Biochem. J. **308:**697–711.
59. **Prinz, S., E. S. Hwang, R. Visintin, and A. Amon.** 1998. The regulation of Cdc20 proteolysis reveals a role for APC components Cdc23 and Cdc27 during S phase and early mitosis. Curr. Biol. **8:**750–60.
60. **Schwab, M., A. S. Lutum, and W. Seufert.** 1997. Yeast Hct1 is a regulator of Clb2 cyclin proteolysis. Cell **90:**683–693.
61. **Shirayama, M., A. Toth, M. Galova, and K. Nasmyth.** 1999. APC(Cdc20) promotes exit from mitosis by destroying the anaphase inhibitor Pds1 and cyclin Clb5. Nature **402:**203–207.
62. **Sia, R. A., H. A. Herald, and D. J. Lew.** 1996. Cdc28 tyrosine phosphorylation and the morphogenesis checkpoint in budding yeast. Mol. Biol. Cell **7:**1657–1666.
63. **Skowyra, D., K. L. Craig, M. Tyers, S. J. Elledge, and J. W. Harper.** 1997. F-box proteins are receptors that recruit phosphorylated substrates to the SCF ubiquitin-ligase complex. Cell **91:**209–219.
64. **Skowyra, D., D. M. Koepp, T. Kamura, M. N. Conrad, R. C. Conaway, J. W. Conaway, S. J. Elledge, and J. W. Harper.** 1999. Reconstitution of G_1 cyclin ubiquitination with complexes containing SCF^{Grr1} and Rbx1. Science **284:**662–665.
65. **Solomon, M. J., and P. Kaldis.** 1998. Regulation of CDKs by phosphoryla-

tion, p. 79–109. *In* M. Pagano (ed.), Cell cycle control, vol. 22. Springer-Verlag KG, Berlin, Germany.
66. **Soos, T. J., M. Park, H. Kiyokawa, and A. Koff.** 1998. Regulation of the cell cycle by CDK Inhibitors, p. 111–131. *In* M. Pagano (ed.), Cell cycle control, vol. 22. Springer-Verlag KG, Berlin, Germany.
67. **Sorger, P. K., and A. W. Murray.** 1992. S-phase feedback control in budding yeast independent of tyrosine phosphorylation of p34^{cdc28}. Nature **355:**365–368.
68. **Spellman, P., G. Sherlock, M. Zhang, V. Iyer, K. Anders, M. Eisen, P. Brown, D. Botstein, and B. Futcher.** 1998. Comprehensive identification of cell cycle-regulated genes of the yeast *Saccharomyces cerevisiae* by microarray hybridization. Mol. Biol. Cell **9:**3273–3297.
69. **Sudakin, V., D. Ganoth, A. Dahan, H. Heller, J. Hershko, F. C. Luca, J. V. Ruderman, and A. Hershko.** 1995. The cyclosome, a large complex containing cyclin-selective ubiquitin ligase activity. Mol. Biol. Cell **6:**185–197.
70. **Tanaka, S., and H. Nojima.** 1996. Nik: A Nim1-like protein kinase of *S. cerevisiae* interacts with the Cdc28 complex and regulates cell cycle progression. Genes Cell **1:**905–921.
71. **Thuret, J.-Y., J.-G. Valay, G. Faye, and C. Mann.** 1996. Civ1 (CAK in vivo), a novel Cdk-activating kinase. Cell **86:**565–576.
72. **Tinker-Kulberg, R. L., and D. O. Morgan.** 1999. Pds1 and Esp1 control both anaphase and mitotic exit in normal cells and after DNA damage. Genes Dev. **13:**1936–1949.
73. **Verma, R., R. S. Annan, M. J. Huddleston, S. A. Carr, G. Reynard, and R. J. Deshaies.** 1997. Phosphorylation of Sic1p by G1 Cdk required for its degradation and entry into S-phase. Science **278:**455–460.
74. **Vidal, M., R. K. Brachmann, A. Fattaey, E. Harlow, and J. D. Boeke.** 1996. Reverse two-hybrid and one-hybrid systems to detect dissociation of protein-protein and DNA-protein interactions. Proc. Natl. Acad. Sci. USA **93:**10315–10320.
75. **Visintin, R., S. Prinz, and A. Amon.** 1997. *CDC20* and *CDH1*: a family of substrate-specific activators of APC-dependent proteolysis. Science **278:**460–463.
76. **Yamamoto, A., V. Guacci, and D. Koshland.** 1996. Pds1p is required for faithful execution of anaphase in the yeast, *Saccharomyces cerevisiae*. J. Cell Biol. **133:**85–97.
77. **Yamamoto, A., V. Guacci, and D. Koshland.** 1996. Pds1p, an inhibitor of anaphase in budding yeast, plays a critical role in the APC and checkpoint pathway(s). J. Cell Biol. **133:**99–110.
78. **Zachariae, W., and K. Nasmyth.** 1999. Whose end is destruction: cell division and the anaphase-promoting complex. Genes Dev. **13:**2039–2058.
79. **Zachariae, W., M. Schwab, K. Nasmyth, and W. Seufert.** 1998. Control of cyclin ubiquitination by CDK-regulated binding of Hct1 to the anaphase promoting complex. Science **282:**1721–1724.
80. **Zachariae, W., T. H. Shin, M. Galova, B. Obermaier, and K. Nasmyth.** 1996. Identification of subunits of the anaphase-promoting complex of *Saccharomyces cerevisiae*. Science **274:**1201–1204.
81. **Zou, H., T. J. McGarry, T. Bernal, and M. J. Kirschner.** 1999. Identification of a vertebrate sister-chromatid separation inhibitor involved in transformation and tumorigenesis. Science **285:**418–422.